The Plant Cell, Vol. 19: 46–62, January 2007, www.plantcell.org © 2007 American Society of Plant Biologists

The *indeterminate gametophyte1* Gene of Maize Encodes a LOB Domain Protein Required for Embryo Sac and Leaf Development[W]

Matthew M.S. Evans[1]

Department of Plant Biology, Carnegie Institution of Washington, Stanford, California 94305

Angiosperm embryo sac development begins with a phase of free nuclear division followed by cellularization and differentiation of cell types. The *indeterminate gametophyte1* (*ig1*) gene of maize (*Zea mays*) restricts the proliferative phase of female gametophyte development. *ig1* mutant female gametophytes have a prolonged phase of free nuclear divisions leading to a variety of embryo sac abnormalities, including extra egg cells, extra polar nuclei, and extra synergids. Positional cloning of *ig1* was performed based on the genome sequence of the orthologous region in rice. *ig1* encodes a LATERAL ORGAN BOUNDARIES domain protein with high similarity to *ASYMMETRIC LEAVES2* of *Arabidopsis thaliana*. A second mutant allele of *ig1* was identified in a noncomplementation screen using active *Mutator* transposable element lines. Homozygous *ig1* mutants have abnormal leaf morphology as well as abnormal embryo sac development. Affected leaves have disrupted abaxial–adaxial polarity and fail to repress the expression of meristem-specific *knotted-like homeobox* (*knox*) genes in leaf primordia, causing a proliferative, stem cell identity to persist in these cells. Despite the superficial similarity of *ig1-O* leaves and embryo sacs, ectopic *knox* gene expression cannot be detected in *ig1-O* embryo sacs.

INTRODUCTION

The plant life cycle has genetically active diploid and haploid phases, called the sporophyte and gametophyte, respectively. In green algae, such as *Ulva lactuca*, the two phases of the life cycle are morphologically similar. During land plant evolution, the extent of the gametophyte phase has become reduced. In primitive land plants, such as the bryophyte *Physcomitrella patens*, the gametophyte is the dominant phase of the life cycle and contains a leafy-shoot phase called the gametophore with at least superficial similarity to the vegetative shoots of seed plants, whereas the sporophyte is greatly reduced and dependent on the gametophyte (Cove and Knight, 1993). In seedless vascular plants such as ferns, the sporophyte is dominant and grows as a leafy shoot, whereas the gametophyte is free-living but greatly reduced and lacking a leafy-shoot phase (Banks, 1999). The gametophytes are smallest in angiosperms, consisting of only a few cells dependent on the sporophyte for growth and development.

The female gametophyte, or embryo sac, undergoes a stereotypical number of divisions to produce an eight-nuclei syncytium. The migration and position of these nuclei are highly regular. The embryo sac then cellularizes to produce four cell types: synergids, antipodals, an egg cell, and a homodiploid central cell (Drews and Yadegari, 2002). In wild-type maize (*Zea mays*), the antipodal cells are the only embryo sac cells that proliferate after cellularization. In *Arabidopsis thaliana*, there is no proliferation after cellularization of the embryo sac, as the antipodals degenerate during maturation (Murgia et al., 1993).

Recently, many mutations have been identified that act genetically during the haploid phase in angiosperms (Ebel et al., 2004; Johnson et al., 2004; Pagnussat et al., 2005). *indeterminate gametophyte1* (*ig1*) in maize is unique among mutants that act in the haploid gametophytes; mutants are viable and have an increased number of nuclei before cellularization of the embryo sac (Huang and Sheridan, 1996; Ebel et al., 2004). *retinoblastoma-related1* (*rbr1*) in *Arabidopsis* is the only other mutant reported with extra rounds of free nuclear divisions, but unlike *ig1*, it also affects the male gametophyte, and *rbr1* embryo sacs do not produce viable progeny.

In *ig1* mutant embryo sacs, the proliferative phase is prolonged, suggesting that wild-type *ig1* function promotes the switch from proliferation to differentiation in the embryo sac (Lin, 1978, 1981; Huang and Sheridan, 1996). Consequently, mutant *ig1* embryo sacs contain extra egg cells, extra central cells, and extra polar nuclei within central cells (Figure 1). The phenotypes of *ig1* mutant embryo sacs suggest a position-based determination of cellular identity (Lin, 1978, 1981; Guo et al., 2004). The ability of the extra cells and nuclei to function as egg cells or polar nuclei, for example, appears to depend on their position in the embryo sac. Because of their abnormal structure, many of these defective embryo sacs give rise to abnormal seeds, which allowed the identification of the *ig1-O* reference allele (Figure 1B). These abnormalities include polyembryony, heterofertilization, miniature endosperms, and early abortion of seeds (Kermicle, 1971). Maize endosperm development is very sensitive to a deviation from the normal 2 maternal:1 paternal genome ratio in the endosperm. Consequently, when an embryo sac with three polar nuclei is fertilized by a standard haploid pollen grain, the

[1] To whom correspondence should be addressed. E-mail mmsevans@stanford.edu; fax 650-325-6857.

The author responsible for distribution of materials integral to the findings presented in this article in accordance with the policy described in the Instructions for Authors (www.plantcell.org) is: Matthew M.S. Evans (mmsevans@stanford.edu).

[W] Online version contains Web-only data.

www.plantcell.org/cgi/doi/10.1105/tpc.106.047506

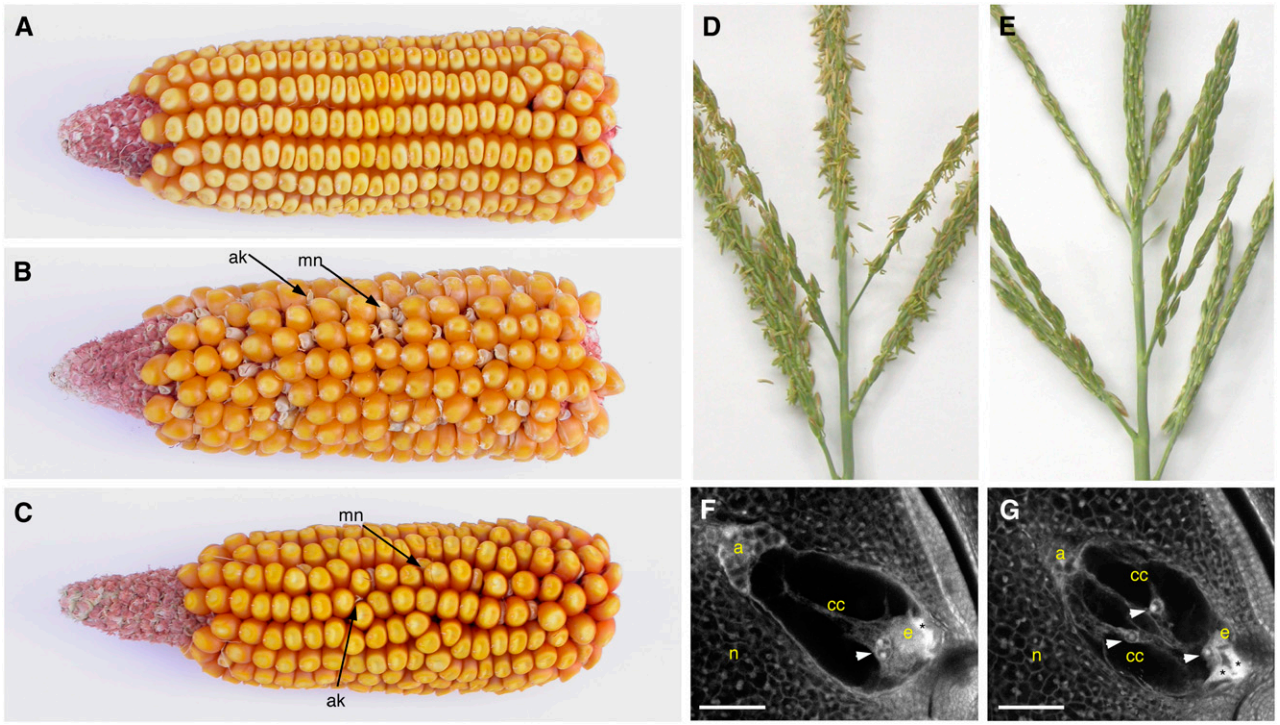

Figure 1. Phenotypes of *ig1* Mutants.

(A) Ear from a W64A wild-type plant.
(B) Ear from an *ig1-O/ig1-O* W64A mutant plant.
(C) Ear from an *ig1-mum/ig1-mum* W64A plant.
(D) Fertile wild-type tassel with anthers extruded.
(E) Sterile *ig1/ig1* mutant tassel without extruded anthers.
(F) Wild-type embryo sac.
(G) *ig1* embryo sac.
Asterisks indicate degenerated synergids. Arrowheads point to polar nuclei. a, antipodal cells; ak, aborted kernel; cc, central cell; e, egg cell; mn, miniature kernel; n, nucellus. Bars = 25 μm.

resulting endosperm is miniature, and when an embryo sac with four or more polar nuclei is fertilized by a haploid pollen grain, the resulting endosperm aborts early in development and collapses (Lin, 1984). This leads to abnormal endosperm development when embryo sacs with extra polar nuclei are fertilized.

Because *ig1* embryo sacs are frequently viable, homozygous lines can be established to examine the role of *ig1* in sporophyte development. Homozygous mutants for *ig1-O* reportedly have normal vegetative morphology but in some genetic backgrounds have sporophytic male sterility, even though there is no gametophytic affect on pollen, either failing to shed pollen or extrude anthers (Kermicle, 1994).

Additionally, *ig1* restricts the embryogenic potential of cells that lack one of the two parental genomes, so that mutant embryo sacs produce haploid progeny, of both maternal and paternal origin, at a higher rate than wild-type embryos (Kermicle, 1969). Paternal haploid production has been used in maize breeding to transfer germplasm from one variety of maize to the cytoplasm of another variety (e.g., a male sterility conditioning cytoplasm) (Kindiger and Hamann, 1993). The ability to produce embryos without a paternal genetic contribution bears some resemblance to apomixis, the production of seeds that are clones of the mother plant (Grimanelli et al., 2001); understanding *ig1* may provide further insight into the development of apomictic plants.

Comparisons of genetic maps and DNA sequences demonstrate a significant conservation of gene order between maize and rice (Moore et al., 1995). *ig1* was cloned by taking advantage of the conserved gene order between maize and rice in the *ig1* region. This report describes the cloning of the *indeterminate gametophyte1* gene and the phenotype of *ig1-O* and a second mutant allele, *ig1-mum*, which affect leaf development as well as embryo sac development. The phenotype of *ig1* plants suggests that common mechanisms control the switch from proliferation to differentiation in both the gametophyte and sporophyte of angiosperms.

RESULTS

The Phenotype of *ig1-O* Is Affected by Genetic Background

The *ig1-O* mutation was backcrossed three to five times to different inbred lines and then pollinated to test the effect of

genetic background on the frequency of mutant phenotypes (Table 1). The A158 inbred line was the most severe, with the highest degree of prefertilization failure of *ig1* mutant embryo sacs and the lowest frequency of normal seeds. The W23 inbred line in which *ig1-O* was first identified had the highest frequency of seeds arising from embryo sacs with extra polar nuclei (miniature and aborted seeds), and W64A gave the next highest frequency for these classes along with A158. Interestingly, although Mo17 was a moderate background with regard to most phenotypic classes, it produced the highest percentage of kernels with more than one embryo (i.e., embryo sacs with more than one egg cell). B73 and W22 suppressed the *ig1-O* seed phenotypes the most. Interestingly, the presence of the homozygous male-sterile phenotype did not correlate with the severity of *ig1* seed phenotypes, suggesting that different loci modify the sporophytic and gametophytic phenotypes of *ig1*.

Identifying a Second Allele of *ig1*

A noncomplementation screen for the male-sterile phenotype of *ig1-O* (Figure 1) was used to identify a second mutant allele, *ig1-mum*, from an active *Mutator* (*Mu*) transposable element line. An active *Mu* line was established in the inbred W64A, because *ig1-O* homozygotes are male-sterile as W64A inbreds and W64A/W23 hybrids. Crosses were made between *ig1-O/ig1-O* W23 females and *Mu* W64A males. Rare male-steriles from an F1 population of 60,000 individuals were crossed as females with standard W64A inbred plants. The progeny of the selections were tested for *ig1* mutant phenotypes. Specifically, these plants were tested for seed phenotypes similar to those of *ig1-O* (i.e., miniature seeds, twins, and aborted seeds) and retested for their failure to complement the male-sterile phenotype of *ig1-O*. By these criteria, one of these selections was shown to carry a new mutant allele of *ig1*, named *ig1-mum*. In addition to causing a male-sterile phenotype in transheterozygotes with *ig1-O* or as homozygotes, *ig1-mum* causes the same abnormal seed types as *ig1-O*, suggesting that the same embryo sac defects are present in *ig1-mum* mutants as in *ig1-O*. Most of the mutant classes occur at a lower frequency in *ig1-mum* than in *ig1-O*, suggesting that *ig1-mum* is a weaker allele in the embryo sac (Figure 1, Table 1).

Fine Mapping and Cloning of *ig1*

Fine mapping of *ig1* was initiated in a population segregating *ig1-O* from a cross between *ig1-O*^{w23}/+^{Mo17} females and +/+Mo17 males. Fine mapping of *ig1* against available simple sequence repeat markers placed *ig1* between *umc1311* and *umc1973* on chromosome 3 of maize. The rice orthologs of the markers around *ig1* were identified by BLAST search for each sequence against the rice genome using the Gramene database for comparative grass genomics (www.gramene.org) (Ware et al., 2002). The orthologs of *umc1311* and *umc1973* on rice chromosome 1 are ~845 kb apart (Figure 2). By generating mapping populations among multiple inbred lines (between *ig1-O* in a W23 inbred background and wild-type Mo17, W64A, A158, or M14), polymorphisms were found with the *umc1539* simple sequence repeat marker that further reduced this interval in the rice map to 378 kb covered by three rice BAC clones.

The Gramene database, in which cDNA and genomic clones of many grasses, including maize, are aligned with their predicted rice orthologs, was used to develop more maize mapping markers. Maize ESTs and methyl-filtered library clones that were orthologs of the rice genes in this interval were used to design PCR primers to generate additional mapping markers. These markers reduced the interval carrying the potential rice ortholog of *ig1* to a 65-kb region containing 12 annotated genes.

A *Mu* insertion in the *ig1-mum* allele in a maize gene orthologous to the rice gene *Os01g66590*, a gene within the 65-kb interval of the rice genome described above, was identified by PCR amplification using a primer for the *Mu* terminal inverted repeat and a gene-specific primer. Additionally, a small population of 24 individuals segregating for the *ig1-mum* allele was used to test for a cosegregating *Mu* band using a modified amplification of insertion mutagenized sites protocol (Frey et al., 1998). One band that cosegregated with *ig1-mum* contained a *Mu*

Table 1. Phenotypic Severity of *ig1-O* and *ig1-mum*

	Normal Endosperm		Absent or	Miniature Endosperm		Aborted/	Ovules	
	One Embryo	Two or More Embryos	Abnormal Embryo	One Embryo	Two or More Embryos	Collapsed Endosperm	without Seeds	Homozygous Phenotype
ig1-O								
A158 (656)	**24**	3	1	13	1	12	46	Male-fertile
W23 (845)	**34**	2	3	9	0	25	27	Male-sterile
W64A (793)	**46**	6	2	7	1	18	20	Male-sterile
Mo17 (948)	**53**	11	2	6	2	11	15	Male-sterile
B73 (792)	**62**	1	2	1	0	7	27	ND
W22 (989)	**72**	0	0	2	1	2	24	Male-fertile
ig1-mum								
Mo17 (775)	**70**	4	3	3	2	3	15	Variable male sterility

Values shown are percentages of mutant ovules. Values shown in boldface represent normal seeds. Numbers in parentheses indicate total ovules (with and without seeds) examined. Inbred lines are ordered from the most to the least severe based on lowest to highest frequency of normal seed production (i.e., highest to lowest penetrance of combined ovule failure and seed defects). ND, not determined.

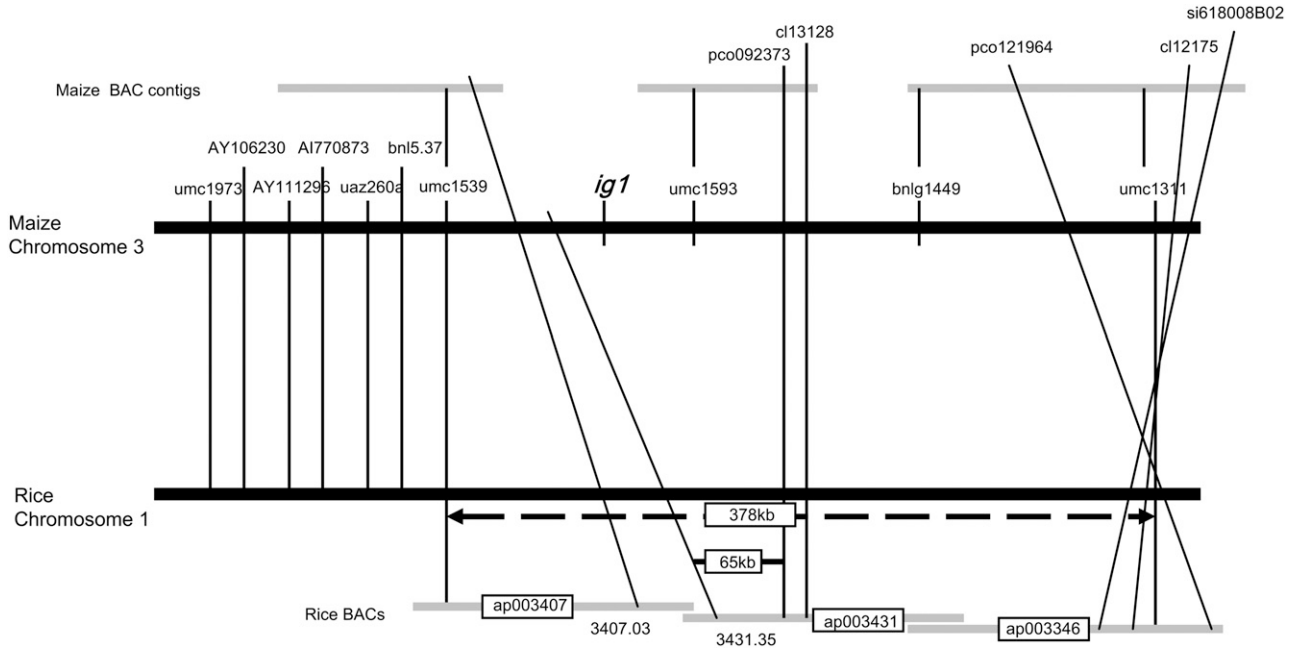

Figure 2. Comparative Mapping between Rice and Maize around *ig1*.

BAC clones and maize BAC contigs are stippled. Arrows indicate the physical distance between markers on rice chromosome 1. Vertical lines show the positions of the closest sequence matches in the rice genome for maize clones in the *ig1* region. Maize markers shown above the maize BACs had been placed on the BAC clones but not on the genetic map. Underlines indicate PCR-based markers designed using rice genome information.

insertion in the assembled *Zea mays* contig, AZM4_49905, orthologous to *Os01g66590* that was used to design primers for the directed *Mu* search described above. This gene encodes a member of the LATERAL ORGAN BOUNDARIES (LOB) protein family, a plant-specific gene family with 43 members in *Arabidopsis* (Iwakawa et al., 2002; Shuai et al., 2002).

Both *ig1-mum* and *ig1-O* were compared along with their progenitors by DNA gel blot hybridization of a probe for the LOB domain of the *ig1* gene (probe 2-4 in Figure 3) with the DNA of heterozygous mutant and homozygous wild-type plants (data not shown). Both alleles have a novel band not present in their progenitors. The *ig1-mum* allele contains a *Mu8* insertion within the first intron, 86 nucleotides upstream of the start codon, and the *ig1-O* allele contains a *Hopscotch* retrotransposon insertion within codon 120 of *ig1*, 14 residues before the end of the LOB domain (Figure 3). *Hopscotch* is one of a group of low-copy retrotransposons that are more commonly inserted into genes than the high-copy retroelements that make up the bulk of the maize genome(White et al., 1994). The *ig1* gene contains four exons that constitute an mRNA 1264 bases in length (Figure 3). The structures of *ig1*, *Oryza sativa ig1* (*Osig1*), and the closest maize homolog to *ig1*, *ig1/as2-like1* (*ial1*), are very similar, with three introns in the same positions.

To test the effect of both *ig1-O* and *ig1-mum* on *ig1* mRNA levels, RT-PCR was performed on whole ear primordia of homozygous *ig1-O* and *ig1-mum* and the wild type (Figure 3). Primers flanking the insertion in either *ig1-mum* or *ig1-O* were used for the RT-PCR experiments. Both *ig1-mum* and *ig1-O* cause a significant decrease in the levels of normal *ig1* mRNA, as measured by amplification around the first intron and the *ig1-mum Mu8* insertion site. There is a 10-fold decrease in the amount of *ig1* message in *ig1-O* and in *ig1-mum*, as measured by quantitative real-time PCR around intron 1. In the *ig1-mum* samples, melting curve and gel analyses demonstrate that most of this PCR product is of abnormal size. Quantitative RT-PCR downstream of the *ig1-mum* insertion site using primers flanking intron 2 and the *ig1-O Hopscotch* insertion site detects a twofold reduction in *ig1* RNA in *ig1-mum* and a 100-fold reduction in *ig1-O*.

Presumably, the discrepancy between the findings for the two pairs of primers in *ig1-mum* results from the presence of many mRNAs in *ig1-mum* ears that have 5′ untranslated regions that are too long to amplify under the conditions used. Sequencing of the RT-PCR products from *ig1-mum* ears obtained with longer extension times revealed that mutant transcripts retained a variable amount of both the first intron and the *Mu8* element. This alteration in the 5′ untranslated region could have affects on the translation efficiency of these messages, even though the abundance of *ig1* message 3′ of the *Mu* insertion is only mildly affected.

ig1 Encodes a LOB Domain Protein Similar to *AS2*

The LOB domain protein encoded by *ig1* has high similarity to that of *ASYMMETRIC LEAVES2* (*AS2*) of *Arabidopsis* (Figure 4). An alignment was made between the proteins encoded by *ig1*, its nearest maize homologs, the entire families of *LOB DOMAIN/AS2-LIKE* (*LBD/ASL*) genes of rice (36 genes) and *Arabidopsis*

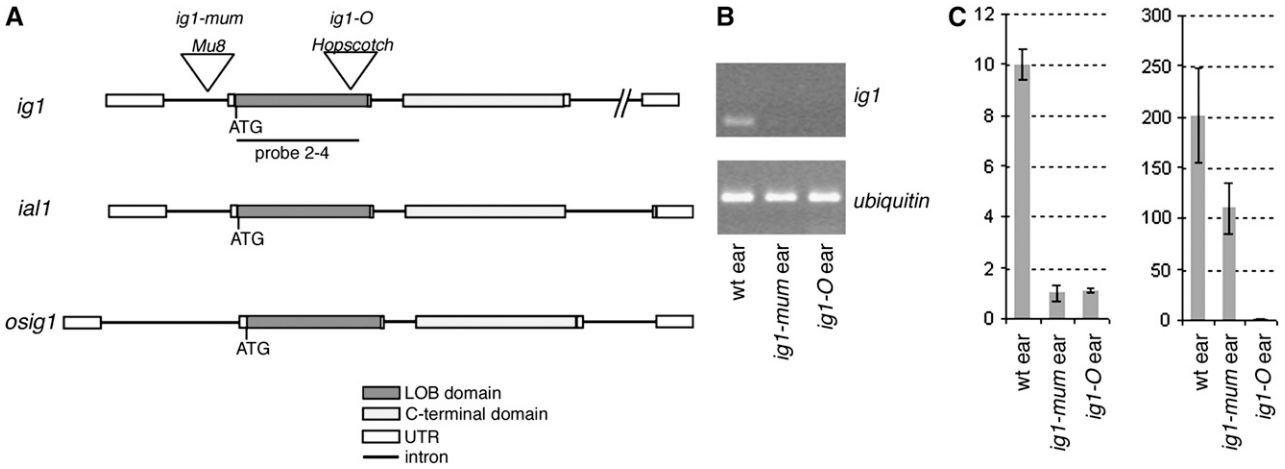

Figure 3. *ig1* Gene Structure and Mutations.

(A) Structures of the *ig1* gene and its rice ortholog. Positions of the *Mu* insertion in *ig1-mum* and the *Hopscotch* insertion in *ig1-O* are indicated. The LOB domain is indicated by dark gray. The first exon contains most of the 5′ untranslated region (UTR); the second exon contains the *LOB* domain; the third exon contains the C-terminal domain; and the fourth exon contains most of the 3′ untranslated region. The third intron is 1.6 kb in length and extends beyond the end of AZM4_49905. The last exon is part of a separate AZM contig, AZM4_116957.

(B) Effect of *ig1* mutations on *ig1* RNA levels. RT-PCR was performed on RNA from whole ear primordia ~5 cm in length using primers for both *ig1* around the first intron and for *ubiquitin* (*ubi*). Lane 1, wild type; lane 2, *ig1-mum* homozygote; lane 3, *ig1-O* homozygote. Homozygous mutants were identified on the basis of male sterility.

(C) Relative *ig1* message levels in *ig1-O* and *ig1-mum* ear primordia normalized to *ubi*. The left graph shows PCR results using primers around the first intron of *ig1* (around the insertion in *ig1-mum* and upstream of the insertion in *ig1-O*), and the right graph shows PCR results using primers around the second intron of *ig1* (downstream of the insertion in *ig1-mum* and around the insertion in *ig1-O*). Error bars indicate SE. Five replicate assays were performed for each pair of PCR primers per sample.

(43 genes), and available *LBD* genes most similar to *AS2* from other plants (Iwakawa et al., 2002; Shuai et al., 2002). Figure 4 shows the portion of this tree encompassing *AS2*, its five closest homologs in *Arabidopsis* (*LBD36*/*ASL1*, *LBD10*/*ASL2*, *LBD25*/*ASL3*, *LOB*/*ASL4*, and *LBD21*/*ASL12*), and *ial* genes from other species. This subclade includes the *ramosa2* (*ra2*) gene of maize, *Sbra2* of *Sorghum bicolor*, and *Osra2* of rice, which are most closely related to *LOB*/*ASL4* of *Arabidopsis* (Bortiri et al., 2006). *ig1* is one of four genes, along with *ial1*, *ial2*, and *ial3*, in maize whose proteins align most closely with that of *AS2*, suggesting substantial redundancy for *AS2* function in maize. There are two rice genes in this clade for the four maize genes (Os *LOB2* and Os *LOB3* [Bortiri et al., 2006], named here Os *ig1* [*Os01g66590*] and Os *ial1* [*Os05g34450*] to reflect their inclusion in the *ig1*/*AS2* subclade of LOB genes), as one would expect based on comparative mapping of grasses and the allotetraploid origin of maize (Gaut and Doebley, 1997). To date, the *AS2* subgroup includes genes from several grasses, including maize, rice, and sorghum (as well as partial sequences of genes from *Hordeum vulgare*, *Triticum aestivum*, and *Saccharum officinarum*; data not shown), one dicot in *Arabidopsis*, and one gymnosperm in *Pinus taeda*.

The members of this clade are distinct from the other LOB domain genes in possessing a SKY motif (often SKYQ) immediately after the LOB domain that is not present in other LOB domain genes in either *Arabidopsis* or rice, even the ASL1, -2, -3, and -4 proteins (Figure 4). These residues immediately follow the last Leu of the predicted Leu zipper coiled-coil domain of the LOB domain. Additionally, the Tyr and Gln residues of the SKYQ motif occupy the g and a positions, respectively, in the Leu zipper after this last Leu. The a, e, and g positions in the helix of Leu zippers determine the specificity of dimerization between Leu zippers (Acharya et al., 2002; Deppmann et al., 2004). Additionally, the presence of a positively charged amino acid in the a position of one of the heptads—Lys in *ig1*, *ial1*, *Sbig1*, *Osig1*, and *AS2* and Arg in *ial2*, *ial3*, and *Osial1*—suggests that these proteins do not homodimerize. This conserved structure suggests that the LOB domain proteins in this clade interact with a conserved partner. The IAL proteins from grass species are distinct from AS2 in *Arabidopsis* in having a longer Ser-rich N-terminal leader upstream of the LOB domain and an Ala-rich sequence downstream of the SKY motif. Whether these are peculiarities of grasses/monocots or are found in other plant LOB proteins cannot be determined until these genes are cloned from more species. Within the LOB domain, IG1 and AS2 are 84% identical; however, the C-terminal domain is not conserved, with only 17% identity between IG1 and AS2. Interestingly, the divergent portion of the protein is in a separate exon from the conserved portion—the LOB domain plus the SKYQ motif—in *ig1* and all grass *IAL* genes for which there are genome sequence data. There is also one gene in the rice genome, *Os02g21390*, that lacks a LOB domain but whose C-terminal half is 60% identical to the C-terminal domain of *ig1* and 76% identical to that of *Osig1*. Based on the protein alignments, there is redundancy of *AS2* gene function in both rice and maize not present in *Arabidopsis*. However, there are also genes in *Arabidopsis* that

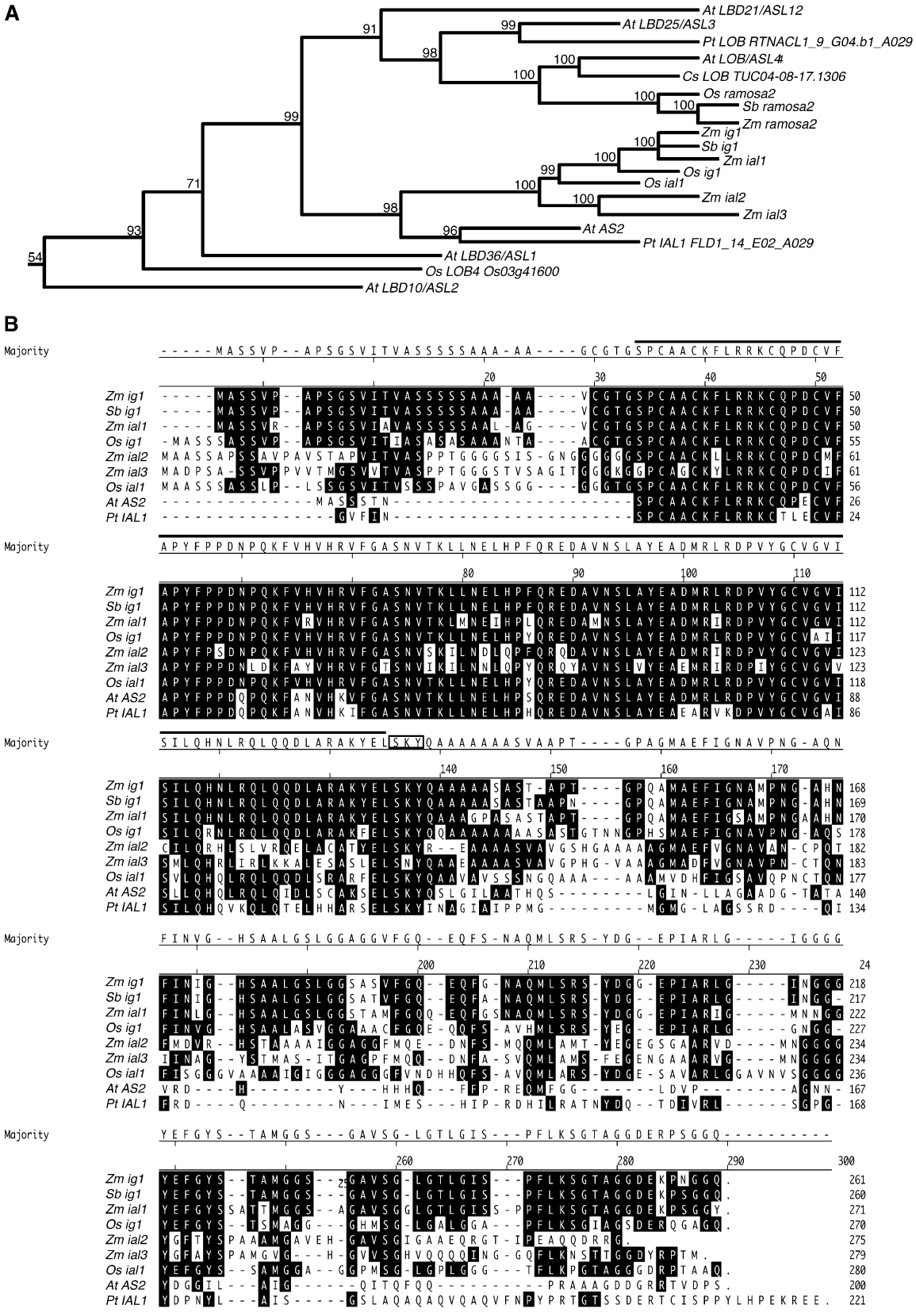

Figure 4. The *ig1* Gene Family.

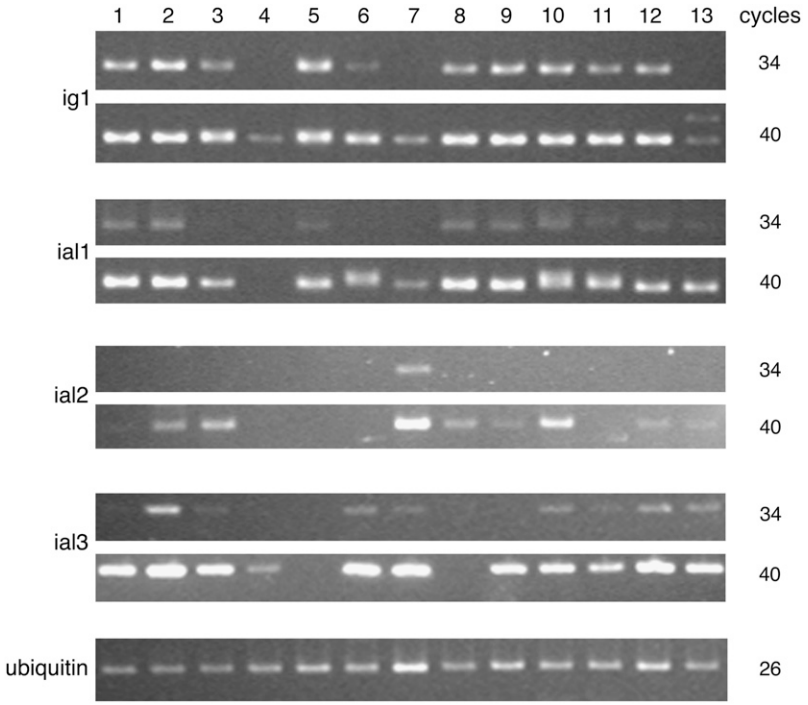

Figure 5. Expression of *ig1* and *ial* Genes in Various Tissues.

RT-PCR was performed on total RNA using *ubi* primers or *ig1* or *ial* primers. Note the larger *ig1* transcript seen after 40 cycles in *ig1-mum* mutant leaves (lane 13). Lane 1, fully expanded leaf; lane 2, immature leaf; lane 3, husk leaf; lane 4, root; lane 5, silk; lane 6, endosperm at 9 d after pollination; lane 7, mature pollen; lane 8, 1-cm-long ear primordium; lane 9, 5-cm-long ear primordium; lane 10, 2-cm-long tassel primordium; lane 11, ovule; lane 12, ligular region of wild-type seedling leaf; lane 13, ligular region of *ig1-mum* flag leaf.

have no clear ortholog in maize or rice, such as *LBD10/ASL2* and *LBD25/ASL3*. Assignment of functional redundancy and orthology, therefore, are tentative without more detailed expression or mutant analysis of these genes.

Expression of *ig1* and Closely Related Genes

ig1 and the *ial* genes are broadly expressed in a variety of tissues in wild-type plants (Figure 5). *ig1* transcript can be detected by RT-PCR in leaves, leaf primordia, immature ears (before and during floret development), immature tassels, whole ovules, silk, and husk leaves. *ig1* has lower expression in endosperm and much lower expression in roots and mature pollen grains. *ial1* is expressed in many of the same tissues but generally at lower levels than *ig1*. *ial2*, unlike *ig1* and *ial1*, has its highest expression in pollen and has very low expression elsewhere. *ial2* RNA levels are too low to be detected in mature leaves, roots, silk, endosperm, or ovules, but it has detectable expression in developing leaves, husks, ears, and tassel primordia. *ial3* is more broadly expressed at higher levels overall than *ial2*. Unlike *ial2*, *ial3* is expressed in ovules and endosperm but is not expressed in young ear primordia. The low expression of *ig1* in pollen grains is consistent with the absence of an effect of *ig1* mutations on the male gametophyte. *ial2* may perform a similar function in the male gametophyte to that of *ig1* in the female gametophyte.

To gain a better understanding of the expression pattern of *ig1* in flowers, in situ hybridization was performed on sections of female flowers from the ear. A probe for the last 33 codons and the 3′ untranslated region was used to reduce the amount of cross-hybridization to *ial1*. Flowers at several stages were examined to detect *ig1* in embryo sacs and floral organs. *ig1* is expressed in the adaxial domain of all organs examined (Figure 6). *ig1* mRNA is found on the adaxial side of lemmas and paleas (sepals), glumes (bracts), and silk (fused carpels) surrounding the

Figure 4. (continued).

(A) Relationship of IG1 with other closely related LOB domain proteins. Only the portion of the LOB domain protein family including AS2 and its five most closely related homologs from *Arabidopsis* is shown. Of the rice and maize genes and the full-length LOB domain genes from a few other species, only those that fall into this same LOB domain subfamily are included. The number above each branch corresponds to the posterior probability for that node.
(B) Alignment of proteins within the IG1/AS2 subgroup. Residues identical to IG1 are highlighted. The LOB domain is indicated by a black line over the residues, and the SKY motif is boxed. The translation start of the *P. taeda* gene is unknown. *Zm*, *Zea mays*; *Sb*, *Sorghum bicolor*; *Os*, *Oryza sativa*; *At*, *Arabidopsis thaliana*; *Pt*, *Pinus taeda*; *Cs*, *Citrus sinensis*.

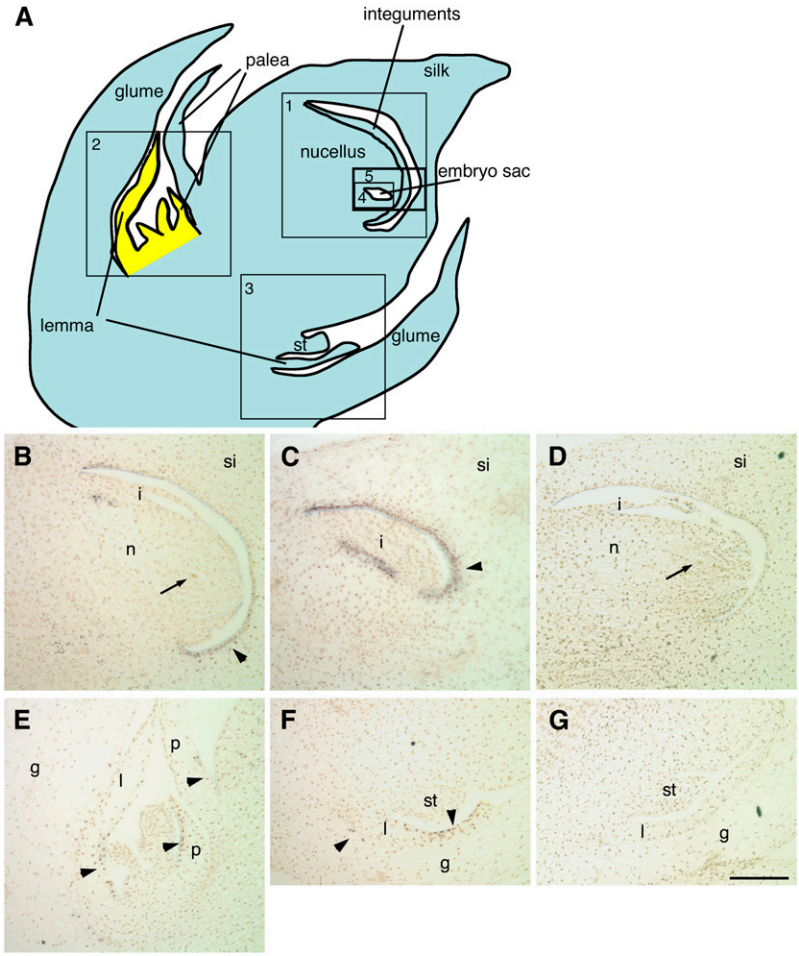

Figure 6. Expression of *ig1* in Floral Organs.

(A) Diagram of a maize female spikelet with a fully developed upper floret and an arrested lower floret (yellow). In a median section, the lemma and palea (the first-whorl organs), one of the arrested stamens, and the silk (gynoecium) with a single ovule can be seen. The area in box 1 is shown in **(B)**, **(C)**, and **(D)**. The area in box 2 is shown in **(E)**. The area in box 3 is shown in **(F)** and **(G)**. The area in box 4 is shown in Figures 7A to 7C. The area in box 5 is shown in Figures 7D to 7H.

(B) and **(D)** Median longitudinal sections of wild-type ovules.

(C) Longitudinal section through the margin of a wild-type ovule. *ig1* is expressed in the adaxial epidermis at the base of the carpels that make up the silk as well as at the boundary between the integuments and the nucellus.

(E) The lower floret and the palea of the upper floret.

(F) and **(G)** The lemma of the upper floret and the inner glume (bract).

Probes were as follows: **(B)**, **(C)**, **(E)**, and **(F)**, *ig1* antisense probe; **(D)** and **(G)**, *ig1* sense probe. Arrowheads point to adaxial expression of *ig1* in floral organs and bracts. Arrows point to embryo sacs. g, glume; i, integument; l, lemma; n, nucellus; p, palea; si, silk; st, stamen. Bar = 100 μm.

single ovule. The expression of *ig1* in the adaxial walls of the carpels that make up the silk forms a ring on the inner wall of the ovary surrounding the ovule. This expression is stronger in the lateral regions of the ovary wall than in the medial domain (Figure 6C). Additionally, *ig1* is expressed at the boundary between the integuments and the nucellus of the ovule (Figures 6B and 6C). The expression on the adaxial side of floral organs becomes restricted to the basal portion of this domain and eventually fades, becoming more difficult to detect as the flowers age. This decrease in *ig1* message is evident in the difference between the adaxial sides of the paleas of the upper and lower florets, because the lower floret is arrested at an earlier stage of development than the upper floret (Figure 6E).

In embryo sacs, *ig1* message is detectable as early as the one-nucleus stage (Figure 7A) but is not detectable in the nonfunctional megaspores. In older embryo sacs, *ig1* message is highest in antipodal cells (Figure 7D). In older embryo sacs, the background staining becomes more intense even with a sense probe for *ig1* (Figure 7H). Consequently, it is difficult to determine whether *ig1* expression continues at these later stages. In particular, it is difficult to determine whether *ig1* expression decreases as embryo sacs age, as it does in lateral organs. Expression in most of the

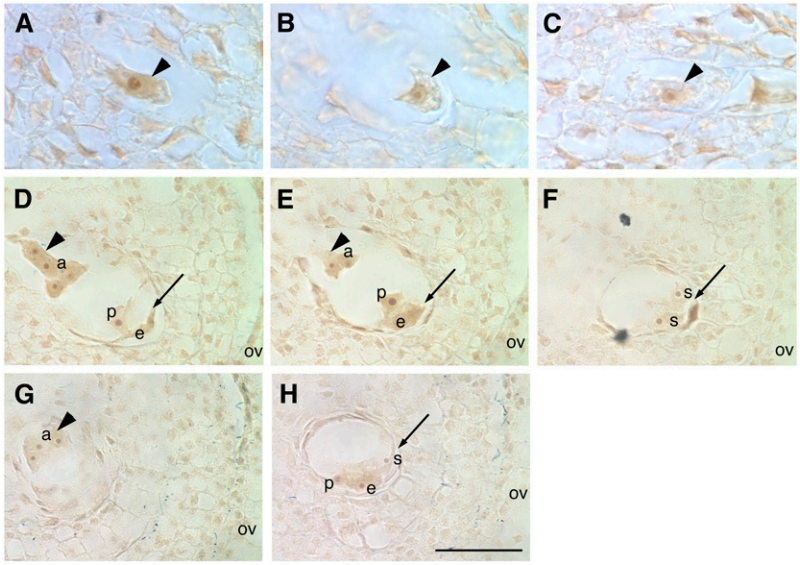

Figure 7. Expression of *ig1* in Embryo Sacs.

(A) to **(C)** Ovules with stage 1 (one-nucleus) embryo sacs.
(A) and **(C)** Wild-type stage 1 embryo sacs (arrowheads). The *ig1* antisense probe detects message in stage 1 embryo sacs.
(B) Nonfunctional megaspore (arrowhead) lacking *ig1* expression from the same ovule as the embryo sac in **(A)**.
(D) to **(H)** Ovules with immature cellularized embryo sacs. Arrowheads point to chalazal nuclei and cells of embryo sacs, and arrows point to micropylar nuclei and cells of embryo sacs.
Probes were as follows: **(A)**, **(B)**, **(D), (E)**, and **(F),** *ig1* antisense probe; **(C)**, **(G)**, and **(H)**, *ig1* sense probe. Signal with the *ig1* antisense probe is higher than that with the sense probe control in the antipodal cells. In the cells at the micropylar end of the embryo sac, the signal is more variable and the background staining with the sense probe is higher, making it difficult to determine whether there is any *ig1* signal. a, antipodal cell; e, egg; ov, ovary wall; p, polar nucleus; s, synergid. Bar = 25 μm for **(A)** to **(C)** and 50 μm for **(D)** to **(H)**.

micropylar cells is frequently not above background. However, *ig1* appears to be expressed in the developing egg cell, and staining around the polar nuclei is also detected occasionally. *ig1* expression is not detected in the developing synergids, however. Therefore, *ig1* may have asymmetric expression within the embryo sac, as it does in lateral organs.

ig1 Controls Leaf Development

The *AS2* gene has been shown to repress the expression of the *knotted1-like homeobox* (*knox*) genes *KNAT1/BREVIPEDICELLUS1* (*BP1*), *KNAT2*, and *KNAT6* in leaf primordia (Ori et al., 2000; Semiarti et al., 2001). During vegetative development, the initiation of lateral organ primordia from an undifferentiated stem cell population is associated with the downregulation of *knox* genes (Jackson et al., 1994; Long et al., 1996). *knox* genes are normally expressed in the shoot apical meristem and excluded from leaf primordia. In maize leaves with ectopic *knox* gene expression, differentiation fails to progress properly and regions of the leaf overproliferate, producing outgrowths and abnormal boundaries between leaf domains (Muehlbauer et al., 1997). In severe cases of *knox* misexpression, leaf cells revert to a stem cell identity and shoot apical meristems develop on the adaxial surfaces of leaves (Sinha et al., 1993).

In *Arabidopsis*, *knox* genes are ectopically expressed in leaf primordia in *as2* mutants (Ori et al., 2000; Semiarti et al., 2001; Iwakawa et al., 2002). Ectopic *knox* gene expression in leaf primordia is also caused by mutations in *rough sheath2* (*rs2*) in maize and *AS1* in *Arabidopsis*, which have been shown to be functionally orthologous, *myb* domain–containing *ARP* (for *AS1 RS2 Phantastica*) genes (Schneeberger et al., 1998; Timmermans et al., 1999; Tsiantis et al., 1999; Byrne et al., 2000; Ori et al., 2000; Semiarti et al., 2001; Iwakawa et al., 2002; Theodoris et al., 2003). No effect of a mutation in a maize *LOB* domain gene on leaf development has been reported previously.

To analyze the effects of *ig1-mum* on sporophyte development, *ig1-mum* heterozygotes were self-pollinated after having been backcrossed three generations to inactive *Mu* W64A and one generation to inactive *Mu* Mo17 inbreds. Interestingly, plants with abnormal morphology of the flag leaf (the last vegetative leaf) were segregating in families segregating *ig1-mum* (Figure 8). The plants in these families were tested for the *ig1-mum* mutation by PCR. All of the plants with leaf abnormalities were *ig1-mum* homozygotes (19 of 19). However, not all *ig1-mum* homozygotes had abnormal flag leaves (i.e., the phenotype was not completely penetrant). In the W64A/Mo17 hybrid background examined, only 19 of 28 homozygotes had abnormal leaf morphology. The incomplete penetrance may reflect a segregation of modifiers that were introduced from either the W64A or Mo17 inbred. Because of this phenotype in *ig1-mum* homozygotes, *ig1-O* homozygotes in a W64A inbred background were examined for leaf defects and discovered to have a similar flag leaf phenotype

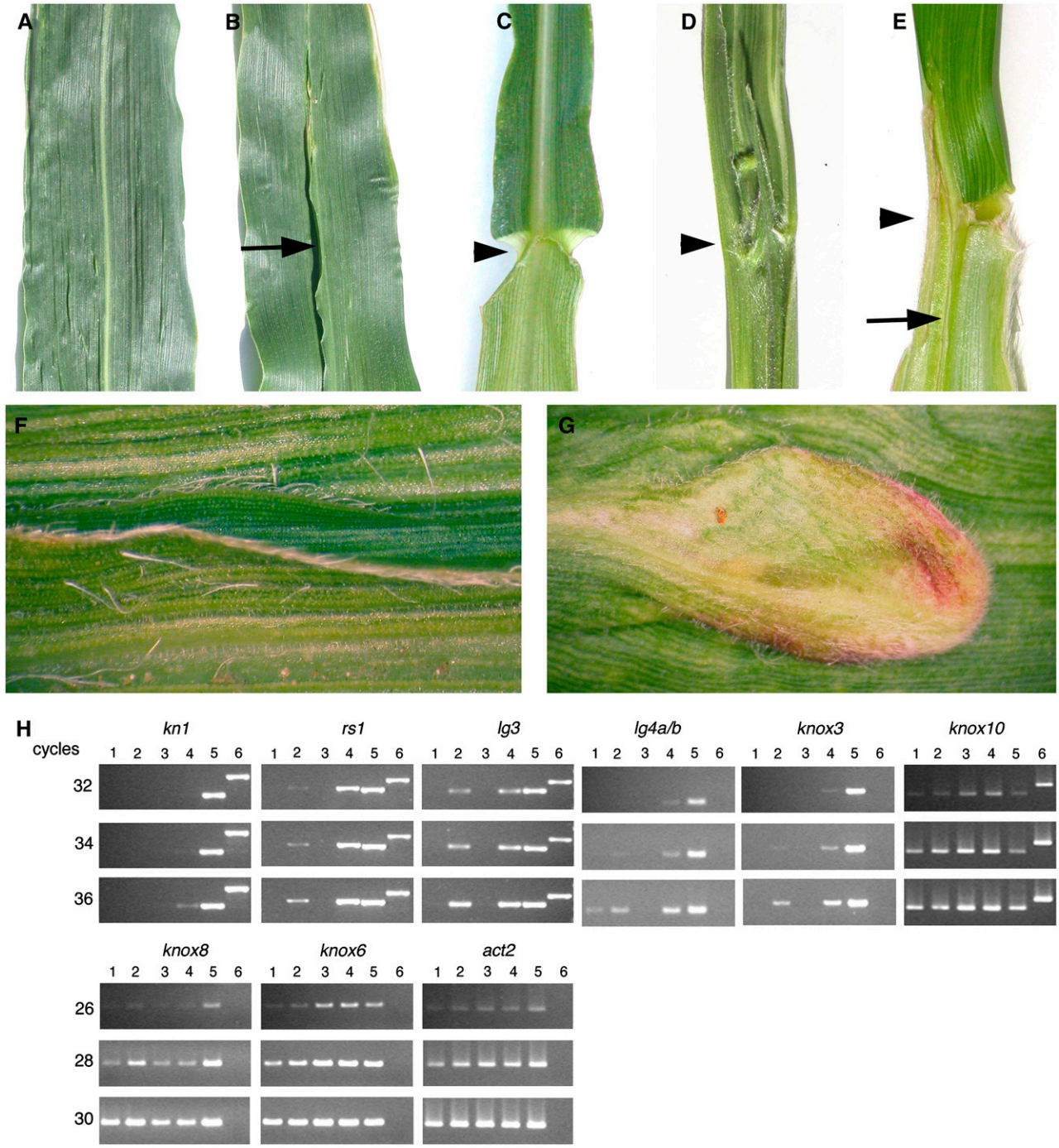

Figure 8. Phenotype of the Flag Leaf (Last Vegetative Leaf) in *ig1/ig1* Homozygotes.

(A) and **(C)** Wild type.
(B), **(D)**, **(F)**, and **(G)** *ig1-mum/ig1-mum*.
(E) *ig1-O/ig1-O* W23.
(A) and **(B)** Adaxial side of the middle of the leaf blade.
(C) to **(E)** Adaxial ligular region. The arrow points to the leaf flap along the midrib. Arrowheads point to the ligular region.
The leaf in **(B)** shows the most common phenotype in *ig1-mum* plants. The leaf in **(D)** shows the most severe *ig1-mum* leaf phenotype. The leaf in **(E)** shows the most common *ig1-O* flag leaf phenotype in a W23 inbred background, with leaf flaps on the sheath and mild ligule distortion.
(F) Close-up of leaf flaps on the adaxial surface of an *ig1-mum* leaf. Note that there are epidermal hairs on the outer epidermis of the flaps but not the inner surfaces of the flaps. The edges of the flaps also have hairs, like normal leaf margins.

as that of *ig1-mum. ig1-O* W64A homozygotes have leaf flaps on the adaxial side of the midrib of the leaf blade, a phenotype not previously reported in homozygous *ig1-O* lines in other inbred backgrounds. Additionally, closer examination of *ig1-O* homozygotes in the original W23 inbred line revealed that most but not all homozygotes (10 of 14) had flag leaves with leaf flaps on the adaxial side of the leaf sheath but not the leaf blade, with occasional disruption of the ligular region (Figure 8E).

Although incompletely penetrant, the most common leaf phenotype of *ig1* mutants is ectopic outgrowths of leaf lamina on the adaxial side of the midrib. The dominant maize mutant *Lax midrib1-O* (*Lxm1-O*) has similar flaps of tissue on either side of the midrib (Schichnes et al., 1997; Schichnes and Freeling, 1998). In contrast with *ig1*, the flaps in *Lxm1-O* are on the abaxial side of the leaf and have adaxial tissue between them, the opposite polarity of that in *ig1*. Some *ig1-mum* mutants have distortions of the ligular region at the boundary between the proximal leaf sheath and the distal leaf blade, a phenotype that more closely resembles that of *rs2* mutants, although these distortions are often associated with leaf flaps on the adaxial sheath (Figure 8). The leaf defects also include rare knots of sheath tissue in the leaf blade (Figure 8G).

To test whether these leaf phenotypes are associated with ectopic *knox* gene expression, RT-PCR was performed on RNA extracted from the ligular region of *ig1-mum* mutant leaves with abnormal leaf morphology as well as *rs2* mutant leaves and wild-type ear primordia as positive controls (Figure 8H). The effect of *ig1-mum* was tested on all class I *knox* genes, *knotted1* (*kn1*), *roughsheath1* (*rs1*), *liguleless3* (*lg3*), *lg4a/b*, *knox3*, *knox8*, *knox10*, and *gnarley1* (*gn1*), as well as on a class II *knox* gene, *knox6*. Ectopic expression of *kn1*, *rs1*, *lg3*, *lg4a/b*, *gn1*, and *knox3* was detected in *ig1-mum* and *rs2* leaves; *knox6*, *knox10*, and possibly *knox8* were unaffected by *ig1-mum*. No ectopic *knox* gene expression was detected in *ig1-mum* seedling leaves, which are normal in appearance (data not shown). These results demonstrate that *ig1-mum* affects many but not all class I *knox* genes and expand the number of *knox* genes known to be affected by *rs2* to include *lg4* and *knox3*. Additionally, they show that not all class I *knox* genes are repressed in leaf primordia; *knox10* has equivalent levels of expression in wild-type leaf and ear primordia, and *knox8* nearly so.

ig1-mum mutant leaves also have defects in abaxial–adaxial polarity. The leaf flaps along the midrib are usually found in pairs and have hairs and sclerenchymal cells on their margins typical of normal leaf margins (Figures 8 and 9). The epidermis of these flaps lacks macrohairs (i.e., is abaxial) on the inner surfaces toward the midrib and has macrohairs (i.e., is adaxial) on the outer surfaces that are continuous with the adaxial surface of the normal leaf lamina (Figure 8F). The switch in leaf polarity includes the internal layers of the leaf as well (Figure 9). In the wild type, the midrib contains large clear cells on the adaxial side of the vasculature and small sclerenchyma cells on the abaxial side. In *ig1-mum* flag leaves, the cells immediately adaxial to the midvein between the two ectopic leaf flaps are sclerenchyma cells typical of the abaxial side of the wild-type leaf, and the adaxial clear cells are absent. The polarity of the vascular bundle in the midrib is not affected. In wild-type leaves, the phloem is located on the abaxial side and the xylem is located on the adaxial side of the veins, and the polarity of cell types within the midvein is normal in *ig1-mum*. Just outside of the two leaf flaps, polarity is normal, with the clear cells present on the adaxial side. Therefore, the leaf flaps appear to be bordered by adaxial tissue on the marginal side and abaxial tissue on the midrib side. The vascular bundles in the leaf flaps also show the same polarity as the macrohairs on the surface. In the *ig1-mum* leaf flaps, the abaxial phloem cells are on the midrib side and the adaxial xylem cells are on the margin side.

This morphology has been seen in other leaf polarity mutants, such as *phantastica* in snapdragon (*Antirrhinum majus*), in which ectopic leaf flaps form at the juxtaposition of adaxial and abaxial tissues (Waites and Hudson, 1995). *as2* loss-of-function mutants in *Arabidopsis* have also been shown to have polarity defects, similar to *ig1-mum*, with abaxial tissue on the adaxial surfaces of leaves, particularly in double mutants with either *erecta* or *rna-dependent rna polymerase6* (Xu et al., 2003; Li et al., 2005). In approximately half of the *ig1-mum* leaves that have these leaf flaps, the abaxial side of the midrib opposite the flaps has a file of epidermal hairs (i.e., is adaxial in character), demonstrating a switch of leaf epidermal identity rather than the duplication of abaxial identity in *as2* mutants or of adaxial identity in dominant *phabulosa1-d* mutants (McConnell et al., 2001). Although this is different from the affect of *as2* in *Arabidopsis*, a similar difference was seen between dominant polarity mutants in the maize *rolled leaf1* gene and those in its homologs in *Arabidopsis*, *REVOLUTA* and *PHABULOSA* (Nelson et al., 2002; Juarez et al., 2004).

Expression of *knox* Genes in Embryo Sacs

The molecular identity of *ig1* and the phenotype of *ig1-mum* leaves suggested that the *ig1* embryo sac phenotype may be caused by ectopic expression of *knox* genes. To test this model, embryo sacs were isolated from homozygous wild-type W23 plants and homozygous *ig1-O* W23 mutant plants. The W23 inbred background was chosen because of its strong expression of the *ig1-O* mutant embryo sac phenotype. Ovules were hand-dissected from developing ears and subjected to digestion with cell wall–degrading enzymes. Embryo sacs were dissected out of ovules with some nucellus cells still attached.

In the ovules used, wild-type embryo sacs had recently cellularized and antipodal cells were not finished proliferating (similar in stage to the embryo sacs shown in Figures 7D to 7H).

Figure 8. (continued).

(G) Knot protruding from the abaxial surface of an *ig1-mum* flag leaf, with anthocyanin and abaxial epidermal hairs typical of sheath tissue.
(H) Expression of *knox* genes in *ig1-mum* and *rs2*. PCR was performed on cDNA from the ligular region of a wild-type flag leaf (lane 1), the ligular region of an *ig1-mum* flag leaf (lane 2), the ligular region of wild-type seedling leaves (lane 3), the ligular region of *rs2* seedling leaves (lane 4), ear primordia (lane 5), or genomic DNA (lane 6).

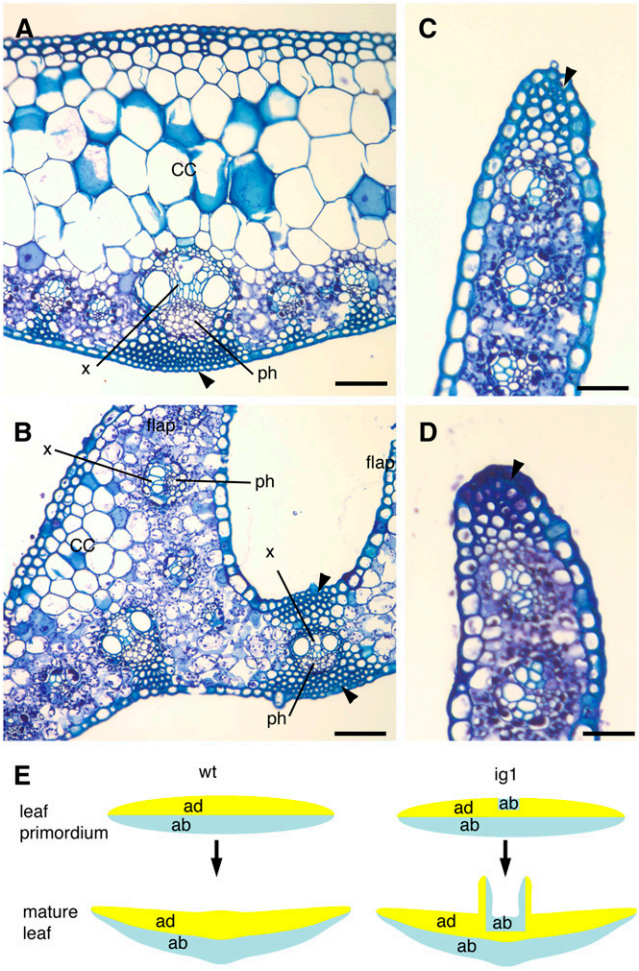

Figure 9. Polarity Defects in *ig1* Flag Leaves.

(A) Midrib of a wild-type flag leaf. The arrowhead points to abaxial sclerenchyma.
(B) Midrib and flaps of an *ig1-mum* flag leaf. Arrowheads point to abaxial and adaxial sclerenchyma.
(C) Normal leaf margin. Arrowhead points to marginal sclerenchyma.
(D) Margin of an *ig1-mum* leaf flap. Arrowhead points to marginal sclerenchyma.
(E) Model of adaxial and abaxial domains in wild-type and *ig1* leaves.
cc, clear cells; ph, phloem; x, xylem. Bars = 150 μm.

The *ig1-O* embryo sacs from similarly staged ovules were much more variable in size and developmental stage. Three replicates were isolated for each genotype, and each replicate contained 13 to 15 embryo sacs. Because of the small amount of RNA isolated from each sample, linear amplification of RNA was performed before quantitative real-time RT-PCR. As a positive control for the ability to detect RNA after linear amplification for each of the primer combinations used, RNA from *rs2* leaves and 5-cm-long wild-type ears used previously and shown in Figure 8 was also subjected to linear amplification and RT-PCR in the same manner as the embryo sac samples. PCRs were repeated at least three times for each pair of PCR primers for each sample. Quantitative real-time PCR was terminated after 61 cycles.

By the end of each run, cDNAs of *ubi* (data not shown) as well as *actin1* (*act1*) and *knox6* (a class II *knox* gene) (Figure 10A) were detected in all embryo sac samples. A second actin gene termed *act2* was consistently expressed in wild-type embryo sacs but was rarely detected in *ig1-O* mutant embryo sacs. Most class I *knox* genes were not consistently amplified from either wild-type or *ig1-O* embryo sacs. *kn1*, *gn1*, *lg4a/b*, and *knox10* were never detected in any embryo sac samples. *rs1*, *lg3*, and *knox3* were seen in only a few PCR samples (2 of the 9 to 12 replicates) after 61 cycles, and for *rs1* and *lg3* only in the wild type. The only class I *knox* gene consistently detected in either wild-type or *ig1-O* embryo sacs was *knox8*. Interestingly, *knox8* RNA levels were greatly reduced in *ig1-O* embryo sacs compared with wild-type sacs. No *knox* genes were overexpressed in *ig1-O* embryo sacs. Additionally, the organ polarity gene *rolled leaf1* was examined in these samples and detected in all mutant and wild-type samples. Expression of *kn1* and *lg3* was also examined in sections of wild-type and *ig1-O* embryo sacs using immunolocalization and in situ hybridization, respectively. Neither *kn1* nor *lg3* showed any difference in expression pattern between mutant and wild-type embryo sacs before or after cellularization (data not shown).

Quantitative analysis was performed for all of the genes—*act1*, *knox6*, *rld1*, *act2*, and *knox8*—that were consistently detected in all wild-type samples. Multiple PCR replicates were performed for each gene. All PCR replicates and biological samples of the same genotype were averaged together and normalized to *ubi* (Figure 10B). *act1*, *knox6*, and *rld1* were expressed at similar levels in *ig1-O* and wild-type embryo sacs. By contrast, there was at least a 100-fold reduction in detectable *act2* and *knox8* message in *ig1-O* embryo sacs compared with wild-type sacs at this stage. The effect of *ig1* mutations on *act2* and *knox8* did not occur in all tissues; mRNA levels of both genes were not significantly different in whole 5-cm-long ear primordia of *ig1-O* and *ig1-mum* homozygotes compared with wild-type primordia (Figure 10C). Additionally, *act2* expression was not altered in *ig1-mum* flag leaves (Figure 8H).

DISCUSSION

The failure to limit proliferation in *ig1* embryo sacs leads to a variety of structural defects, including the production of extra gametes and synergids. Additionally, the fertilization process is frequently abnormal, producing seeds with haploid embryos and embryos and endosperms derived from fertilization by different pollen tubes. These late defects have often been interpreted as resulting from the abnormal structure of *ig1* embryo sacs rather than from a requirement for *ig1* in the female gametes per se. The synergids are known to attract pollen tubes (Higashiyama et al., 2001; Huck et al., 2003; Rotman et al., 2003; Marton et al., 2005), and the presence of extra synergids may promote the entry of extra pollen tubes into the embryo sac, leading to heterofertilization. Alternatively, *ig1* may directly prevent these abnormal events by inhibiting embryogenesis in the egg cell until fertilization and karyogamy occur.

Although the leaf phenotype of *ig1* is incompletely penetrant, the molecular identity of the gene, its expression pattern in lateral organs of the flower, and the presence of the phenotype in two independent alleles demonstrate that this phenotype is a

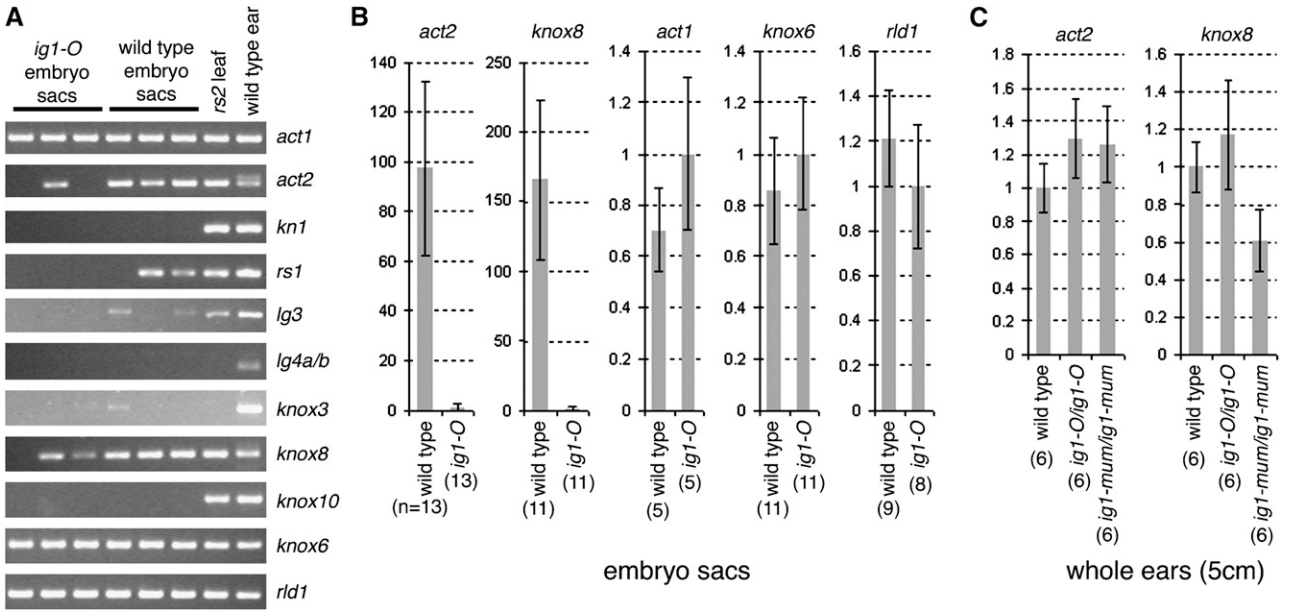

Figure 10. Expression of Genes from Whole Embryo Sacs.

RNA was subjected to linear amplification and then used for quantitative real-time PCR.

(A) Products after the completion of real-time RT-PCR.

(B) Comparison of RNA levels of *act2*, *knox8*, *act1*, *knox6*, and *rld1* in wild-type and *ig1-O* embryo sacs. Expression of *ubi* was used to normalize RNA levels between samples. Expression is given relative to that of *ig1-O*. Because of the dramatic difference between *ig1-O* and wild-type embryo sacs for *act2* and *knox8*, these genes are compared using a log scale, whereas all others are presented on a linear scale.

(C) Relative levels of RNA of *act2* and *knox8* in developing wild-type, *ig1-O*, and *ig1-mum* ear primordia.

Error bars in **(B)** and **(C)** represent SE. The number of replicates is given in parentheses below each column.

consequence of mutation in *ig1*. Genetic background differences, coupled with the subtle phenotype in W23, could explain why this phenotype had not been reported previously, although it may also be dependent on certain growing conditions. The incomplete penetrance of the leaf phenotype in a pure W23 line demonstrates that this variability need not be caused by segregation of modifiers but can reflect either an inherent variability in the development of *ig1* leaves or a dependence of the phenotype on particular environmental conditions.

Both alleles affect only the last one or two vegetative leaves of the plant in all backgrounds tested. The absence of an effect of *ig1-mum* on most leaves of the plant may reflect redundancy with *ial1*, *ial2*, or *ial3* or incomplete loss of *ig1* function in *ig1-mum*. However, *ial1*, *ial2*, and *ial3* are all expressed in flag leaves that have the phenotypes of *ig1-mum*, suggesting that the absence of expression of one of these genes is not responsible for the phenotype in *ig1-mum* flag leaves. Alternatively, there may be qualitative differences between these leaves that make the flag leaves more sensitive to a partial reduction in *ig1/ial* function. For example, the level of expression of *lg4a/b* is higher in wild-type flag leaves than in wild-type seedling leaves (Figure 8H).

AS2 is a nuclear protein that interacts physically with AS1 protein, suggesting a role for *LOB* domain genes in regulating transcription (in the case of *AS2* in combination with *AS1*) (Iwakawa et al., 2002; Xu et al., 2003). IG1 protein (referred to as maize AS2) was recently shown to interact with RS2 in vitro, supporting the model that it also acts as a transcriptional regulator and is orthologous with AS2 (Phelps-Durr et al., 2005). It is not yet known whether AS1 and AS2 repress the transcription of *knox* genes directly or indirectly. Interestingly, regarding the role of *ig1* in restricting the embryogenic potential of cells lacking a maternal or paternal genome, leaf sections from *as2* mutants have an enhanced ability to develop autonomous shoots in vitro compared with wild-type leaves (Semiarti et al., 2001). To date, no effect of *as2* on the *Arabidopsis* embryo sac has been reported.

AS2 mRNA is polarly localized to the adaxial domains of developing cotyledons (Iwakawa et al., 2002). Similarly, *ig1* is expressed in the adaxial domains of lateral organs. This expression is strongest throughout the adaxial domain in early primordia. Later in organ development, this expression is restricted to the basal region and eventually is undetectable in older primordia. Loss of function of *ig1* causes some of the cells in the adaxial domain of the midrib to adopt an abaxial fate. The subsequent juxtaposition of abaxial and adaxial domains leads to the outgrowth of ectopic flaps of leaf lamina flanking the midrib on the upper surface of leaves. These flaps are more commonly found in the basal portion of the leaf and are often associated with disruption of the proximal–distal axis and with distortion of the ligular region as well. Like *as2* mutant leaves, *ig1* flag leaves also have ectopic expression of *knox* genes.

In embryo sacs, *ig1* is expressed at low levels as early as the one-nucleus stage. The early time of *ig1* expression in embryo sacs is consistent with an early role for *ig1* in embryo sac

development. After studying the effects of *ig1-O* in an embryonic marker line, Enaleeva et al. (1998) concluded that *ig1* acts as early as the first division of the embryo sac and affects the establishment of polarity and the subsequent progression of nuclear divisions and cytokinesis (Enaleeva et al., 1998). Later in embryo sac development, expression is even lower and is near the threshold for detection, but it appears to be higher at the chalazal end. The *ig1* loss-of-function phenotype, like the leaf phenotype, may be caused by a partial loss of polarity in the embryo sac, and the later defects, including prolonged proliferation, are consequences of this defect.

However, not all aspects of the leaf and embryo sac phenotypes in *ig1* are similar. There are no *knox* genes overexpressed in *ig1-O* mutant embryo sacs after cellularization, although ectopic expression of one or more *knox* genes in a brief period of embryo sac development cannot be completely ruled out. Two genes, *knox8* and *act2*, have been identified, however, with reduced expression in *ig1-O* embryo sacs. The fact that *ig1* does not affect these genes in the same way in other tissues suggests that they are not direct targets of *ig1* but instead are associated with the morphological defects of *ig1* embryo sacs. One explanation is that these genes are normally expressed in maturing embryo sacs and *ig1-O* delays the switch from proliferation to maturation programs, thereby suppressing their expression. Alternatively, *knox8* and *act2* may be expressed asymmetrically in the embryo sac, and this pattern is disrupted in *ig1* mutants.

The molecular identity of *ig1* and the phenotype of *ig1* mutant leaves suggested that common mechanisms had been used in switching from proliferation to differentiation in gametophytic (embryo sac) and sporophytic (lateral organ primordia) tissues. *ig1* function may reflect ancestral homology between gametophyte and sporophyte shoot development. In this case, an *ig1-like* LOB gene in conjunction with an *ARP* gene imposes determinacy by negatively regulating *knox* genes in both gametophyte and sporophyte development. In primitive land plants, such as *Physcomitrella patens*, the gametophyte is the dominant phase of the life cycle and contains a leafy-shoot phase called the gametophore with at least superficial similarity to the vegetative shoots of seed plants (Cove and Knight, 1993). However, there is currently no evidence that *ig1* interacts with the same partners or affects the expression levels of the same genes in embryo sacs and lateral organ primordia.

Another possible explanation is that *ig1* function in the female gametophyte is a later adaptation and is not derived from ancestral gametophyte function. This adaptation may have occurred at any of several points in plant gametophyte evolution. For example, the adoption of *ig1* for gametophyte development may have occurred in basal angiosperm lineages to limit the growth of the gametophyte, or it may have occurred in only a subset of angiosperm lineages. Basal angiosperms are thought to have been four-nuclei-type, and the eight-nuclei Polygonum type arose from an early duplication event along the micropylar–chalazal axis, making a domain of nuclei at the chalazal end as well as the micropylar end of the embryo sac. *ig1* may function to restrict this to a single duplication event, and in *ig1* mutants the process is reiterated. In basal angiosperms, *ig1* genes may act to prevent this duplication entirely, and a slight modification in *ig1* function or timing led to this duplication in plants with the Polygonum type of megagametogenesis. Additionally, *ig1* function in the embryo sac may have been adopted to restrict proliferation in the postcellularization phase to the antipodal cells in angiosperms, such as maize, in which the antipodals proliferate. *knox* genes do not seem to be repressed by *ig1* in embryo sacs as they are in leaves. Instead, *ig1* likely controls the expression of other downstream genes that promote proliferation in the embryo sac. Whether these genes are also affected in mutant leaves is unknown.

Alternatively, the C-terminal domain of the IG1 protein may be critical for *ig1* function in the embryo sac, whereas the LOB domain is critical for lateral organ function. The C-terminal domain of AS2 is different from that of IG1 and perhaps does not confer a function in the embryo sac, which would explain the lack of any reported effect of *as2* mutations on embryo sac development. Interestingly, there appears to be a gene in rice and putatively also in maize that has this C-terminal domain but lacks an N-terminal LOB domain, suggesting that the C-terminal domain may have a separate molecular function. By contrast, there are no genes in *Arabidopsis* with high similarity to this domain.

The analysis of these processes in lower plant gametophytes with more extensive development will help elucidate whether *ig1* function in leaves and embryo sacs arose through conservation of an ancestral mechanism in gametophytes and sporophytes or through the convergence of the mechanisms regulating sporophyte and gametophyte development. Finally, changes in the timing and expression pattern of *ig1* orthologs within the gametophyte may have led to changes in the duration of the haploid phase of the plant life cycle in higher plants.

METHODS

Genetics

Maize (*Zea mays*) plants were grown in summer field conditions or in greenhouses in 16-h-light/8-h-dark conditions. To identify a new allele of *ig1*, active *Mu*; *r1*; W64A plants were crossed as males onto male-sterile *ig1-O*/*ig1-O*; *R1-navajo* (*R1-nj*) females in either a W23 inbred or a W23/W64A hybrid genetic background. The *ig1-O* mutation is on a W23 chromosome. A total of 60,000 F1 individuals were screened for male sterility (failure to extrude anthers). Male-sterile individuals were pollinated as females by standard *r1*; W64A males. Maternal haploids were distinguished based on their shorter stature, and maternal diploids and *ig1-O* sibling pollen contaminants were distinguished by homozygosity for *R1-nj*. Eight male-sterile individuals heterozygous for *R1-nj* were identified. The progeny of these plants were tested for markers linked to *ig1* to identify individuals homozygous for W64A alleles (i.e., not carrying *ig1-O*^{w23}). Only one line had *ig1* seed phenotypes when pollinated by standard W64A pollen, demonstrating the presence of a new *ig1* mutant allele designated *ig1-mum*.

ig1 fine mapping was performed simultaneously in four different populations. *ig1-O*^{w23} was crossed with one of the following inbred lines: Mo17, W64A, A158, and M14. The F1 plants were backcrossed as females by the appropriate inbred line. *ig1-O* individuals were identified as seeds with miniature endosperm or twin embryos. Recombinants were identified as individuals homozygous for the allele of the backcross parent (Mo17, W64A, A158, or M14). Rare androgenetic progeny that arise in *ig1-O* resemble recombinants, as they also have lost the W23 allele for that particular marker, but are distinguished by their apparent

homozygosity at all loci. PCR conditions were as described previously (Evans and Kermicle, 2001).

Cloning of *ig1*

Identification of a *Mu* insertion in *ig1-mum* was initially identified by PCR using 5′-GTTGTGCTGGAGGATGGAGATGAC-3′ for the *ig1* gene, 5′-TGGCGTTGGCTTCTMTG-3′ as a *Mu* primer, and 5′-GCCTCCATTTCGTCGAATCCC-3′ as a nested *Mu* primer. Amplification of insertion-mutagenized sites was performed using a protocol modified from that of Frey et al. (1998). Approximately 500 ng of DNA was digested per sample with 5 units of *Hin*P1I (New England Biolabs), and then adaptors were ligated overnight using 1 unit of T4 DNA ligase (Fermentas). Sequences of the two strands of the adaptors were 5′-GACCACGCGTATCGATGTCGACGAGATGAGTCCTGAG-3′ and 5′-CGCTCAGGATCCACTCAT-3′. Ligation reactions were diluted 1:1, and 15 μL was used for a first round of PCR in a final volume of 25 μL. The 25-μL reaction mix consisted of 10 μM primers, 2.0 mM $MgCl_2$, 250 μM each deoxynucleotide triphosphate, 10 mM Tris, pH 8.3, 50 mM KCl, 3.0% DMSO, and 0.5 units of Platinum Taq (Invitrogen). First-round PCR was performed with a primer for the adaptor, 5′-GACCACGCGTATCGATGTCGAC-3′, and a primer for the ends of the *Mu* elements, 5′-GAGAAGCCAACGCCAWCGCCTCC-3′, for 30 cycles of 1 min at 94°C, 30 s at 65°C, and 1 min at 72°C. PCRs were performed on a PTC-200 Thermal Cycler (MJ Research). The PCR products were diluted 1:10, and 2.8 μL was used in a 28-μL reaction with the same conditions as the first round except that amplification was performed with 10 cycles of 94°C for 30 s, 66°C for 30 s, and 72°C for 1 min followed by 30 cycles of 94°C for 30 s, 61°C for 30 s, and 72°C for 1 min. Nested primers for the second round of PCR were 5′-GACCACGCGTATCGATGTCGACGAG-3′ for the adaptor and a 5′ Hex-labeled *Mu* primer, 5′-GCCTCCATTTCGTCGAATCCC-3′. PCR products were separated on a 6% denaturing polyacrylamide gel, and the fluorescent bands were visualized on a Typhoon 8600 laser scanner/imager using 532-nm excitation and 580-nm emission. Bands of interest were excised from the gel, macerated, and allowed to elute overnight in TE (10 mM Tris and 1 mM EDTA, pH 8.0). PCR products were reamplified using *Mu* and adaptor primers and cloned into pGEM T-easy (Promega). Multiple clones were sequenced for each band selected.

To identify the lesion in the *ig1-O* allele, genomic DNA of *ig1-O*/+ heterozygote and its wild-type W23 progenitor was digested with *Eco*RI and probed with a fragment of the *ig1* gene encompassing most of the LOB domain. The *ig1-O* mutant had a novel band of ~1.6 kb in length. This band was excised from agarose gels and purified using the Qiagen gel extraction kit. The *ig1-O* fragment was amplified using inverse PCR according to the method of Cowperthwaite et al. (2002) except that the annealing temperature for the PCR was 67°C. Primers used were 5′-GCGGCCGCGGCTGCTGAGGAAGAAGA-3′ and 5′-CCCTTCCAGCGCGAGGACGCCGTGAACT-3′ for the first round of amplification and 5′-GCTGCTGAGGAAGAAGACGACGCCACGGTGATCA-3′ and 5′-CGGCTGCGTCGGCGTCATCTCCATCCT-3′ for the second round. The PCR product was cloned into pGEM T-easy and sequenced. The *Hopscotch* insertion was verified by PCR using a primer for the *Hopscotch* long terminal repeat, 5′-AAATCAAGGAGATCCTGTGCTATCTACGT-3′, and an *ig1* primer upstream of the element, 5′-GTCATCTCCATCCTCCAGCACAAC-3′, and the complement of the *Hopscotch* primer and an *ig1* downstream primer, 5′-AACTCTGCCATCGCTTGCGG-3′, to verify the 3′ end of the insertion.

Gene Expression Analysis

To determine the transcription start and stop sites as well as the intron–exon structure, 5′ and 3′ rapid amplification of cDNA ends was performed using the GeneRacer kit (Invitrogen) according to the manufacturer's directions. For the amplification of the 5′ end of the *ig1* transcript, the first primer was 5′-GGCGCATGTCGGCCTCGTAGGCGAGGGAGTTCA-3′ and the nested primer was 5′-GCGGCCGCGGCTGCTGAGGAAGAAGA-3′. For the amplification of the 3′ end, the first primer was 5′-CGGCTGCGTCGGCGTCATCTCCATCCT-3′ and the nested primer was 5′-TCGGCGTCATCTCCATCCTCCAGCACAACCTACGA-3′. RNA was isolated from tissues using the Trizol reagent (Invitrogen). Genomic DNA was removed using the DNA-free kit (Ambion), and cDNA was synthesized using the Thermoscript RT-PCR system and priming with oligo(dT) (Invitrogen). For RT-PCR of *ig1* cDNA, the primers used were 5′-GCTACGCCAAGGCCCAAGTGT-3′ for exon 1 and 5′-GCACCGACGAAGCCATCC-3′ for exon 2. RT-PCR of *ial1* was performed with the same exon 2 primer as *ig1* and 5′-CGAGTGCCCAGGCATTCTTCAG-3′ for exon 1. RT-PCR primers for *ial2* were 5′-GAACTCGCCTGCGCCACCTAC-3′ and 5′-AGCTCCACTGCCTTCACCTTCGTAG-3′, and primers for *ial3* were 5′-CGCCGTCAATTCGCTCGTTTAC-3′ and 5′-TCGTGGAGTACCCGGCATTGATAA-3′. Primers for *rs1*, *lg3*, and *ubi* were the same as those described by Schneeberger et al. (1998). Primers for *kn1* were 5′-TGGGAACAGCGGCGGTAGC-3′ for exon 1 and 5′-ATCTCCGTCAGCCTCGCCGA-3′ for exon 2. Primers for *lg4a* and *lg4b* were 5′-GCCGCAAGGTGGGMGCG-3′ and 5′-GGCAGTAMGYSTCCATGAAYTCGTCG-3′. Primers for *knox3* were 5′-GCTGCAGCTGCAGATAAAACTGGAGT-3′ and 5′-TCTTCTCCATCTCCGAGGGGTAGG-3′. Primers for *knox6* were 5′-GGCCATACCCAACTGAAGACGACA-3′ and 5′-TGCTCTGGATCAATATCACCTTTTCTTCT-3′. Primers for *knox8* were 5′-GACCCGGAGCTCGACCAGTTCAT-3′ and 5′-ACGACCCGGCGACCTCACAGTTAC-3′. Primers for *knox10* were 5′-CCCGCCAGAAGCTCCTCCACT-3′ and 5′-CCGTGCTGGCCCATCCTGTAAT-3′. Primers for *act2* were 5′-CCTTTCGAAAGTCCTTGCGTCACA-3′ and 5′-GCGAAACCGGCCTTGACCAT-3′. For some genes, at least one of the primers has a binding site that spans the junction between two exons, so it cannot anneal to genomic DNA, thus preventing genomic DNA amplification. For PCR, 40 ng of cDNA was amplified for 26 to 36 cycles of 94°C for 30 s, 65°C for 30 s, and 72°C for 30 s using 1 unit of Taq DNA polymerase (Promega), 200 μM deoxynucleotide triphosphate, and 0.2 μM of each primer.

Identification of Other *LOB* Genes and Phylogenetic Analysis

ial and other *LOB* domain genes from maize and other species were identified by searching EST and Genome Survey Sequence databases at Gramene (www.gramene.org) for rice (*Oryza sativa*); The Institute for Genomic Research (http://maize.tigr.org), Iowa State University (magi.plantgenomics.iastate.edu), and PlantGDB (www.plantgdb.org) for maize; and PlantGDB for other species. The alignment of the full-length proteins of *ig1* and related genes was done using ClustalW. Bayesian phylogenetic analysis was conducted on a Clustal-aligned subset of the full *LOB* domain gene data set (see Supplemental Figure 1 online) using MrBayes version 3.1.2 (Huelsenbeck and Ronquist, 2001). Default settings were used and allowed to run for 100,000 generations. Trees were summarized after discarding the first 25,000 generations.

Embryo Sac Isolation and Gene Expression

Ovules from homozygous wild-type W23 and homozygous *ig1-O* W23 plants were dissected from flowers with silk of ~2 cm in length. Three replicates were isolated for each sample. Thirteen to 15 ovules were collected from a single row of flowers to encompass a few different stages of ovule development. Ovules were placed in an enzyme mix of 0.75% pectinase, 0.5% cellulase, and 0.25% pectolyase in 1× PBS for 1 h. Embryo sacs with some attached nucellus cells were liberated from ovules with tungsten needles and, using a Pasteur pipette, placed immediately in extraction buffer RLT (Plant RNeasy kit; Qiagen). Tissue was homogenized on a Mixer Mill300 (Qiagen) with one tungsten-carbide bead in each tube. Nine to 30 ng of total RNA was then subjected to linear amplification using the RiboAmp kit (Arcturus) according to the

manufacturer's instructions. After amplification, cDNA was made from 150 ng of amplified antisense RNA using random primers and the Thermoscript RT-PCR system (Invitrogen). cDNA products were brought to a final volume of 100 μL, and 1 μL of cDNA was amplified for 61 cycles of 94°C for 15 s, 65°C for 30 s, and 72°C for 30 s. PCR was performed using the DyNAmo enzyme mix (New England Biolabs) on an Opticon2 thermocycler (MJ Research) to allow detection of amplicons in real time. Primers were primarily the same as those used for leaf tissue except that those for *kn1*, *rs1*, *lg3*, *lg4*, and *knox3* were replaced with primers near the 3′ end of transcripts because the RiboAmp products are biased against long fragments and 5′ ends. New primers for embryo sac expression are as follows: for *kn1*, 5′-TCAGAAGGTGGCACTGGCTGAGTCTAC-3′ and 5′-GGTACAGCCCGCCGTCGTTGAT-3′; for *rs1*, 5′-CACTACAAGTGGCCGTACCCTTCAGAGAC-3′ and 5′-ACGGCCCGTCCATGTACAGAGCA-3′; for *lg3*, 5′-GTCCAATTGTGCCTGTATCGAAGTAGAGT-3′ and 5′-CTACGGAGGAAGACAAGGTGAGGCT-3′; for *lg4*, 5′-GGCTGCGGTCCGAGTTCCTG-3′ and 5′-TGTCCTCCGACGGCTTCCAAT-3′; for *knox3*, 5′-CGGAGTCGACGGGGCTGGA-3′ and 5′-ATCCGGCCGGGCGTAGAACA-3′; for *rld1*, 5′-CTGTGCTGCTCCTTTAAGGAGAAACCTA-3′ and 5′-AGGTACGCGTAGCCCTGTTCCATT-3′; and for *act1*, 5′-GAAGTGCGAAGTGCGACGTCGATATCAGGAAGGA-3′ and 5′-TGAGATCCACATCTGTTGGAAGGTGCTC-3′. Quantitative analysis of PCR results was performed using the qBase analysis package for Microsoft Excel.

Histology

Rows of developing florets of different stages were dissected from ears, fixed, embedded in paraffin, and sectioned according to McSteen and Hake (2001). *ig1* cDNA from codon 228 to the end of the 3′ untranslated region was cloned in both orientations in pGEM T-easy (Promega) to get both sense and antisense transcripts driven by the T7 promoter. For both sense and antisense probes, plasmids were digested with *Sal*I, and in vitro transcription reactions performed using the MAXIscript T7 kit (Ambion) according to the manufacturer's instructions with digoxigenin-11-UTP to label probes. In situ hybridizations were performed according to Long and Barton (1998). For histology of leaves, samples were fixed, embedded in paraffin, sectioned, and rehydrated as done for in situ hybridization of florets; sections were then stained for 1 min in 0.2% Toluidine Blue-O.

Accession Numbers

Sequence data from this article can be found in the GenBank data library under accession numbers EF081454 (*ig1*) and EF081455 (*ial1*).

Supplemental Data

The following material is available in the online version of this article

Supplemental Figure 1. Alignment of Proteins Used to Produce the Phylogeny of *ig1* and Closely Related *LOB* Genes.

ACKNOWLEDGMENTS

I thank Jerry L. Kermicle for assistance initiating this project and for valuable discussions. I thank Sarah Hake for anti-KNOTTED1 antibody and M. Kathryn Barton for help with in situ hybridizations. This project was supported by a grant from the National Science Foundation to M.M.S.E.

Received September 18, 2006; revised October 27, 2006; accepted November 13, 2006; published January 5, 2007.

REFERENCES

Acharya, A., Ruvinov, S.B., Gal, J., Moll, J.R., and Vinson, C. (2002). A heterodimerizing leucine zipper coiled coil system for examining the specificity of a position interactions: amino acids I, V, L, N, A, and K. Biochemistry **41:** 14122–14131.

Banks, J.A. (1999). Gametophyte development in ferns. Annu. Rev. Plant Physiol. Plant Mol. Biol. **50:** 163–186.

Bortiri, E., Chuck, G., Vollbrecht, E., Rocheford, T., Martienssen, R., and Hake, S. (2006). ramosa2 encodes a LATERAL ORGAN BOUNDARY domain protein that determines the fate of stem cells in branch meristems of maize. Plant Cell **18:** 574–585.

Byrne, M.E., Barley, R., Curtis, M., Arroyo, J.M., Dunham, M., Hudson, A., and Martienssen, R.A. (2000). Asymmetric leaves1 mediates leaf patterning and stem cell function in Arabidopsis. Nature **408:** 967–971.

Cove, D.J., and Knight, C.D. (1993). The moss *Physcomitrella patens*, a model system with potential for the study of plant reproduction. Plant Cell **5:** 1483–1488.

Cowperthwaite, M., Park, W., Xu, Z., Yan, X., Maurais, S.C., and Dooner, H.K. (2002). Use of the transposon Ac as a gene-searching engine in the maize genome. Plant Cell **14:** 713–726.

Deppmann, C.D., Acharya, A., Rishi, V., Wobbes, B., Smeekens, S., Taparowsky, E.J., and Vinson, C. (2004). Dimerization specificity of all 67 B-ZIP motifs in *Arabidopsis thaliana*: A comparison to *Homo sapiens* B-ZIP motifs. Nucleic Acids Res. **32:** 3435–3445.

Drews, G.N., and Yadegari, R. (2002). Development and function of the angiosperm female gametophyte. Annu. Rev. Genet. **36:** 99–124.

Ebel, C., Mariconti, L., and Gruissem, W. (2004). Plant retinoblastoma homologues control nuclear proliferation in the female gametophyte. Nature **429:** 776–780.

Enaleeva, N.K., Ot'kalo, O.V., and Tyrnov, V.S. (1998). Phenotypic expression of the ig mutation in megagametophyte of the maize line Embryonic marker. Genetika **34:** 259–265.

Evans, M.M.S., and Kermicle, J.L. (2001). Interaction between maternal effect and zygotic effect mutations during maize seed development. Genetics **159:** 303–315.

Frey, M., Stettner, C., and Gierl, A. (1998). A general method for gene isolation in tagging approaches: Amplification of insertion mutagenised sites (AIMS). Plant J. **13:** 717–721.

Gaut, B.S., and Doebley, J.F. (1997). DNA sequence evidence for the segmental allotetraploid origin of maize. Proc. Natl. Acad. Sci. USA **94:** 6809–6814.

Grimanelli, D., Leblanc, O., Perotti, E., and Grossniklaus, U. (2001). Developmental genetics of gametophytic apomixis. Trends Genet. **17:** 597–604.

Guo, F., Huang, B.Q., Han, Y., and Zee, S.Y. (2004). Fertilization in maize indeterminate gametophyte1 mutant. Protoplasma **223:** 111–120.

Higashiyama, T., Yabe, S., Sasaki, N., Nishimura, Y., Miyagishima, S., Kuroiwa, H., and Kuroiwa, T. (2001). Pollen tube attraction by the synergid cell. Science **293:** 1480–1483.

Huang, B.Q., and Sheridan, W.F. (1996). Embryo sac development in the maize indeterminate gametophyte1 mutant: Abnormal nuclear behavior and defective microtubule organization. Plant Cell **8:** 1391–1407.

Huck, N., Moore, J.M., Federer, M., and Grossniklaus, U. (2003). The Arabidopsis mutant feronia disrupts the female gametophytic control of pollen tube reception. Development **130:** 2149–2159.

Huelsenbeck, J.P., and Ronquist, F. (2001). MRBAYES: Bayesian inference of phylogenetic trees. Bioinformatics **17:** 754–755.

Iwakawa, H., Ueno, Y., Semiarti, E., Onouchi, H., Kojima, S., Tsukaya, H., Hasebe, M., Soma, T., Ikezaki, M., Machida, C., and Machida, Y. (2002). The ASYMMETRIC LEAVES2 gene of *Arabidopsis thaliana*, required for formation of a symmetric flat leaf

lamina, encodes a member of a novel family of proteins characterized by cysteine repeats and a leucine zipper. Plant Cell Physiol. **43:** 467–478.

Jackson, D., Veit, B., and Hake, S. (1994). Expression of maize KNOTTED1 related homeobox genes in the shoot apical meristem predicts patterns of morphogenesis in the vegetative shoot. Development **120:** 405–413.

Johnson, M.A., von Besser, K., Zhou, Q., Smith, E., Aux, G., Patton, D., Levin, J.Z., and Preuss, D. (2004). Arabidopsis hapless mutations define essential gametophytic functions. Genetics **168:** 971–982.

Juarez, M.T., Kui, J.S., Thomas, J., Heller, B.A., and Timmermans, M.C. (2004). microRNA-mediated repression of rolled leaf1 specifies maize leaf polarity. Nature **428:** 84–88.

Kermicle, J.L. (1969). Androgenesis conditioned by a mutation in maize. Science **166:** 1422–1424.

Kermicle, J.L. (1971). Pleiotropic effects on seed development of the indeterminate gametophyte gene in maize. Am. J. Bot. **58:** 1–7.

Kermicle, J.L. (1994). Indeterminate gametophyte (ig): biology and use. In The Maize Handbook, M. Freeling and V. Walbot, eds (New York: Springer-Verlag), pp. 388–393.

Kindiger, B., and Hamann, S. (1993). Generation of haploids in maize: A modification of the indeterminate gametophyte (ig) system. Crop Sci. **33:** 342–344.

Li, H., Xu, L., Wang, H., Yuan, Z., Cao, X., Yang, Z., Zhang, D., Xu, Y., and Huang, H. (2005). The putative RNA-dependent RNA polymerase RDR6 acts synergistically with ASYMMETRIC LEAVES1 and 2 to repress BREVIPEDICELLUS and MicroRNA165/166 in Arabidopsis leaf development. Plant Cell **17:** 2157–2171.

Lin, B.-Y. (1978). Structural modifications of the female gametophyte associated with the indeterminate gametophyte (ig) mutant in maize. Can. J. Genet. Cytol. **20:** 249–257.

Lin, B.-Y. (1981). Megagametogenetic alterations associated with the indeterminate gametophyte (ig) mutation in maize. Rev. Bras. Biol. **41:** 557–563.

Lin, B.-Y. (1984). Ploidy barrier to endosperm development in maize. Genetics **107:** 103–115.

Long, J.A., and Barton, M.K. (1998). The development of apical embryonic pattern in Arabidopsis. Development **125:** 3027–3035.

Long, J.A., Moan, E.I., Medford, J.I., and Barton, M.K. (1996). A member of the KNOTTED class of homeodomain proteins encoded by the STM gene of Arabidopsis. Nature **379:** 66–69.

Marton, M.L., Cordts, S., Broadhvest, J., and Dresselhaus, T. (2005). Micropylar pollen tube guidance by egg apparatus 1 of maize. Science **307:** 573–576.

McConnell, J.R., Emery, J., Eshed, Y., Bao, N., Bowman, J., and Barton, M.K. (2001). Role of PHABULOSA and PHAVOLUTA in determining radial patterning in shoots. Nature **411:** 709–713.

McSteen, P., and Hake, S. (2001). barren inflorescence2 regulates axillary meristem development in the maize inflorescence. Development **128:** 2881–2891.

Moore, G., Devos, K.M., Wang, Z., and Gale, M.D. (1995). Cereal genome evolution. Grasses, line up and form a circle. Curr. Biol. **5:** 737–739.

Muehlbauer, G.J., Fowler, J.E., and Freeling, M. (1997). Sectors expressing the homeobox gene liguleless3 implicate a time-dependent mechanism for cell fate acquisition along the proximal-distal axis of the maize leaf. Development **124:** 5097–5106.

Murgia, M., Huang, B.-Q., Tucker, S.C., and Musgrave, M.E. (1993). Embryo sac lacking antipodal cells in *Arabidopsis thaliana* (Brassicaceae). Am. J. Bot. **80:** 824–838.

Nelson, J.M., Lane, B., and Freeling, M. (2002). Expression of a mutant maize gene in the ventral epidermis is sufficient to signal a switch of the leaf's dorsoventral axis. Development **129:** 4581–4589.

Ori, N., Eshed, Y., Chuck, G., Bowman, J.L., and Hake, S. (2000). Mechanisms that control knox gene expression in the Arabidopsis shoot. Development **127:** 5523–5532.

Pagnussat, G.C., Yu, H.J., Ngo, Q.A., Rajani, S., Mayalagu, S., Johnson, C.S., Capron, A., Xie, L.F., Ye, D., and Sundaresan, V. (2005). Genetic and molecular identification of genes required for female gametophyte development and function in Arabidopsis. Development **132:** 603–614.

Phelps-Durr, T.L., Thomas, J., Vahab, P., and Timmermans, M.C. (2005). Maize rough sheath2 and its Arabidopsis orthologue ASYMMETRIC LEAVES1 interact with HIRA, a predicted histone chaperone, to maintain knox gene silencing and determinacy during organogenesis. Plant Cell **17:** 2886–2898.

Rotman, N., Rozier, F., Boavida, L., Dumas, C., Berger, F., and Faure, J.E. (2003). Female control of male gamete delivery during fertilization in *Arabidopsis thaliana.* Curr. Biol. **13:** 432–436.

Schichnes, D., Schneeberger, R., and Freeling, M. (1997). Induction of leaves directly from leaves in the maize mutant Lax midrib1-O. Dev. Biol. **186:** 36–45.

Schichnes, D.E., and Freeling, M. (1998). Lax midrib1-O, a systemic, heterochronic mutant of maize. Am. J. Bot. **85:** 481–491.

Schneeberger, R., Tsiantis, M., Freeling, M., and Langdale, J.A. (1998). The rough sheath2 gene negatively regulates homeobox gene expression during maize leaf development. Development **125:** 2857–2865.

Semiarti, E., Ueno, Y., Tsukaya, H., Iwakawa, H., Machida, C., and Machida, Y. (2001). The ASYMMETRIC LEAVES2 gene of *Arabidopsis thaliana* regulates formation of a symmetric lamina, establishment of venation and repression of meristem-related homeobox genes in leaves. Development **128:** 1771–1783.

Shuai, B., Reynaga-Pena, C.G., and Springer, P.S. (2002). The lateral organ boundaries gene defines a novel, plant-specific gene family. Plant Physiol. **129:** 747–761.

Sinha, N.R., Williams, R.E., and Hake, S. (1993). Overexpression of the maize homeo box gene, KNOTTED-1, causes a switch from determinate to indeterminate cell fates. Genes Dev. **7:** 787–795.

Theodoris, G., Inada, N., and Freeling, M. (2003). Conservation and molecular dissection of ROUGH SHEATH2 and ASYMMETRIC LEAVES1 function in leaf development. Proc. Natl. Acad. Sci. USA **100:** 6837–6842.

Timmermans, M.C., Hudson, A., Becraft, P.W., and Nelson, T. (1999). ROUGH SHEATH2: A Myb protein that represses knox homeobox genes in maize lateral organ primordia. Science **284:** 151–153.

Tsiantis, M., Schneeberger, R., Golz, J.F., Freeling, M., and Langdale, J.A. (1999). The maize rough sheath2 gene and leaf development programs in monocot and dicot plants. Science **284:** 154–156.

Waites, R., and Hudson, A. (1995). phantastica: A gene required for dorsiventrality of leaves in *Antirrhinum majus.* Development **121:** 2143–2154.

Ware, D.H., et al. (2002). Gramene, a tool for grass genomics. Plant Physiol. **130:** 1606–1613.

White, S.E., Habera, L.F., and Wessler, S.R. (1994). Retrotransposons in the flanking regions of normal plant genes: A role for copia-like elements in the evolution of gene structure and expression. Proc. Natl. Acad. Sci. USA **91:** 11792–11796.

Xu, L., Xu, Y., Dong, A., Sun, Y., Pi, L., and Huang, H. (2003). Novel as1 and as2 defects in leaf adaxial-abaxial polarity reveal the requirement for ASYMMETRIC LEAVES1 and 2 and ERECTA functions in specifying leaf adaxial identity. Development **130:** 4097–4107.